EFFECT OF TEST SPECIMEN GEOMETRY ON DUCTILE FRACTURE TOUGHNESS OF A C-Mn STEEL

L. Bauvineau[*] , M. Bethmont[+] , H. Burlet[*,⋆] and A. Pineau[*].

J_R-resistance curves obtained on a C-Mn steel with different specimens are compared. The experiments confirm a geometrical dependence of the fracture toughness. An attempt is made to explain these results in terms of models derived from the local approach to fracture. The first model, based on the critical cavity growth, does not fully predict the variations of J_{1c} values. The second model, based on the mechanics of porous materials, gives results in better agreement with the experiments.

INTRODUCTION

The mechanical integrity of PWR components based on fracture mechanics requires the determination of J_R-curves obtained from laboratory specimens, for example CT or SENB specimens. The original idea was that one unique resistance curve is sufficient to characterize the material. However, there is a growing body of evidence showing that the J_R-curves especially the tearing modulus depend on the specimen size, geometry and loading mode. Moreover, this dependency is different from one material to another. Therefore, the application of the J_R-curves for real structures is questionable. One method to obtain loading and geometry independent material parameters is to model the microscopic process of ductile crack growth. This method is called 'local approach'.

This paper is divided into two main parts. Firstly, we discuss the effect of specimen size, side grooves and geometry effects on the J_R-curves of a C-Mn steel. Secondly, we propose two local approaches based on the Rice & Tracey [1] and Rousselier [2] models f7or the prediction of ductile crack initiation and growth.

[*] Centre des Matériaux - Ecole des Mines de Paris, BP87 91003 Evry (France), URA CNRS 866.
[+] EDF, Direction des Etudes et Recherches, Route de Sens, 77250 Moret sur Loing (France).
[⋆] CEA, DEM/SGM, 17 rue des Martyrs, 38054 Grenoble Cedex 9 (France).

MATERIAL AND EXPERIMENTAL PROCEDURES

▫ *Material*

A C-Mn steel of PWR secondary piping component with a ferritic-pearlitic microstructure was tested at 300°C. Moreover the distribution of MnS and Al_2O_3 inclusions resulting from the relatively high content in sulfur (210ppm wt pct, see **Table 1**) and from the rolling conditions was largely inhomogeneous. The volume fraction of inclusions ,f_v ,was estimated from the chemical composition [3] :

$$f_V = 0.054\left[\%S - \frac{0.001}{\%Mn}\right] + 0.05\%O = 0.15\% \qquad (1)$$

Quantitative metallography was used to measure the inhomogeneity in the distribution of inclusions responsible for the initiation of ductile rupture. This analysis led to a volume fraction of about 0.23% which is not too far from the above result. The mechanical properties at 300°C in the tangential direction are : σ_Y=200MPa, UTS=500MPa, with a work-hardening exponent n≈0.27.

C	Si	Mn	P	S	Cr	Ni	O	Al	N
0.20	0.23	0.97	0.022	0.021	0.10	0.12	0.008	0.007	0.011

TABLE 1 : Chemical composition in weight percent.

▫ *Fracture specimen design*

CT and SENT specimens were used to measure the ductile tearing resistance (J-Δa) of the material. The crack plane was chosen such that the propagates along the rolling direction of the plate. Conventional CT specimens of different thicknesses (12.5, 25 and 50mm) with 20% side grooves and a/W≈0.60 were tested. CT specimens without side grooves (thickness equal to 25mm) were also tested. The SENT specimens had in-plane dimensions of 25x25mm with and without 20% side grooves and a/W=0.35. These specimens were tested under clamped conditions which strongly limitate the rotation.

▫ *Calculation of J*

The J-integral for the CT specimens was evaluated following the ASTM E813-89 procedure. For the SENT specimens (with clamped conditions), the J-integral was estimated from the area (U) under the curve giving the load (P) versus the crack mouth opening displacement (δ) :

$$J = \frac{\eta_\delta U}{B_N (W - a_0)} \qquad (2)$$

where B_N is the specimen net thickness and a_0 is the initial crack length. The η_δ coefficient was determined from FEM simulations [4] :

$$\eta_\delta = 1 + 0.084\ a/W - 1.178\ (a/W)^2 \quad \text{for } 0.1 \le a/W \le 0.6 \text{ and } n \approx 0.27 \qquad (3)$$

The crack extension Δa was measured from direct examinations of the crack surface of the specimens broken at liquid nitrogen temperature after unloading. The J_R-curves were obtained with the 'multiple specimen technique'.

EXPERIMENTAL RESULTS

▫ ***Thickness effect***

The J_R-curves (**Fig. 1**), obtained on CT specimens with 20% side grooves, show that the J_{1c} values are nearly independent of the thickness. However, the crack growth resistance (slope dJ/da) in CT50 specimens is lower than that in CT12.5 and CT25 specimens. The fracture surfaces of the different specimens display delaminations related to the distribution of MnS inclusions as shown in **Fig. 3**. The effect observed on the J_R-curves seems to be relevant to the high inhomogeneity of the inclusion distribution.

▫ ***Side-grooves effect***

The J_R-curves for CT and SENT specimens with a thickness of 25mm are compared in **Fig. 2**. The J_{1c} values for specimens with side grooves are systematically lower (by ≈20%) than those of the specimens without side grooves. The slopes dJ/da are identical for the CT specimens. But for the SENT geometry, the slope dJ/da is higher (≈20%) for the specimens without side gooves.

▫ ***Geometrical effect***

In all cases (with and without side gooves), the J_{1c} values are larger in SENT specimens (by ≈30%) than in CT specimens (**Fig. 2**). The slopes dJ/da are similar except for the SENT specimens without side grooves.

NUMERICAL ANALYSIS

In the present study, we analyse only the case of specimens with side-grooves for which 2D calculations under plane strain conditions can be used. 3D calculations were also made. The results in terms of load-displacement curves are similar between the 3D and 2D calculations with plane strain conditions. The local results are slightly different. **Fig. 4** shows the stress triaxiality ratio at a distance of 700μm ahead from the crack tip. The 3D calculations give variations between the CT and SENT specimens lower than those obtained from 2D calculations. The stress triaxiality ratio, at crack initiation, is about 1.6 for SENT specimens and 2.4 for CT specimens. These results can explain the observed variations of J_{1c} values through models based on the local approach to fracture.

▫ ***Model based on critical cavity growth***

The growth of cavities initiated from inclusions is assumed to obey the Rice and Tracey [1] equation :

$$\ln\left(\frac{R}{R_0}\right)_c = \int_{\varepsilon_0}^{\varepsilon_r} 0.283 \exp\left(\frac{3}{2}\frac{\sigma_m}{\sigma_{eq}}\right) d\varepsilon_{eq}^p \qquad (4)$$

where R is the actual size of the cavities and R_0 their initial size. The initial strain ε_0 corresponding to the nucleation of cavities is assumed to be equal to zero. In equation (**4**) ε_r represents the strain to failure.

The fracture criterion has two independent parameters. The first one is the critical cavity growth ratio $(R/R_0)_c$; the second one is the process zone size ahead of the crack tip. According to the local criterion theory [5], the critical cavity growth ratio has been assessed from tests on notched tensile specimens. Since stress and strain gradients are low in these specimens, the size of the mesh is not an important parameter. The critical cavity growth ratio $(R/R_0)_c$ for the present C-Mn steel was found to be equal to 1.26 [4]. The second parameter is the element size (λ) at the crack-tip. This parameter can be fitted from the results on a given cracked geometry in order to simulate crack initiation. An identification on the results of CT25-specimens with side grooves gives an element size (λ) of 700μm. The values of λ and $(R/R_0)_c$ are then used to predict crack initiation (J_{1c}) for SENT specimens. Full details can be found elsewhere [4].
The predictions from this model are presented in **Fig. 5**. The results show that this type of model tends to predict dependencies of J_{1c} values much larger than those observed : $(J_{1c})^{model} \approx 300 kJ/m^2$ for $(J_{1c})^{exp.} = 130 kJ/m^2$. The delaminations (**Fig. 3**) produce plane stress conditions at the crack tip. To simulate this local condition, calculations were made with a plane stress element at the crack tip and plane strain elements for the rest of the structure. For this new calculation, the element size was λ=400μm. The results (**Fig. 5**) are similar to the 3D calculations or 2D calculations under plane strain conditions.
In this approach, the distribution of the inclusions is considered to be uniform. Actually, optical observations show that the inclusions are inhomogeneously distributed. This distribution must modify the stress field at the crack tip and therefore the predictions of the model. Further work is under progress to account for this effect.

▫ ***Rousselier model***

The Rousselier model [2] defines a porous plastic potential Φ taking into account the damage, through the porosity f. It is defined by the relation :

$$\Phi = \frac{\sigma_{eq}}{(1-f)\sigma_*} + \frac{\sigma_1}{\sigma_*} f D \exp\left(\frac{\sigma_m}{(1-f)\sigma_1}\right) - 1 = 0 \qquad (5)$$

where σ_* is the equivalent stress of an ideal material without damage, D and σ_1 are constant material parameters. Identifications led to : D=1.5, σ_1=190MPa with λ=200μm. The initial volume fraction of cavities f_0 was taken as equal to 0.2%.
This model can be used to simulate the J_R-curves. The simulated and experimental results of the CT and SENT specimens with side-grooves are plotted on **Fig. 6** where it is observed that the geometrical dependency of J is better described. In this model the effect of stress triaxiality on the increase in volume fraction of cavities is slightly different from the effect predicted from **Eq. 4**. This might explain the difference observed between both models.

CONCLUSIONS

Tests carried out on different specimens confirm that J_R-curves are dependent on specimen geometry. In particular the values of J are found to be lower in CT type specimens than in SENT specimens.

Two models based on the local approach for fracture analysis have been used. The first model based on critical cavity growth with a uniform distribution of inclusions is shown to be unable to fully explain the observed geometrical dependence. The second model based on Rousselier potential gives results in better agreement with the experiments.

REFERENCES

[1] J. R. Rice, D. M. Tracey, *J. Mech. and Phys. of Sol., Vol. 17*, 1969, pp. 201-217.

[2] G. Rousselier, *Nucl. Eng. and Design*, Vol. 105, 1987, pp. 97-111.

[3] A. G. Franklin, *J. of The Iron and Steel Institute*, Feb. 1969, pp. 181-186.

[4] L. Bauvineau, H. Burlet, A. Pineau, *internal report EDF-DER/ARMINES, n°T42L33/7DO225/RNE450*, Février 1996.

[5] F. Mudry, F. di Rienzo, A. Pineau, *ASTM STP 995, J. D. Landes et al. (ed.)*, 1989, pp. 24-39.

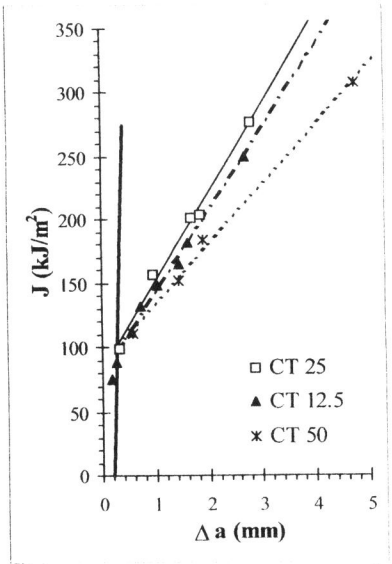

Figure 1 : Size effect on J_R-curves for CT specimens with 20% side-grooves.

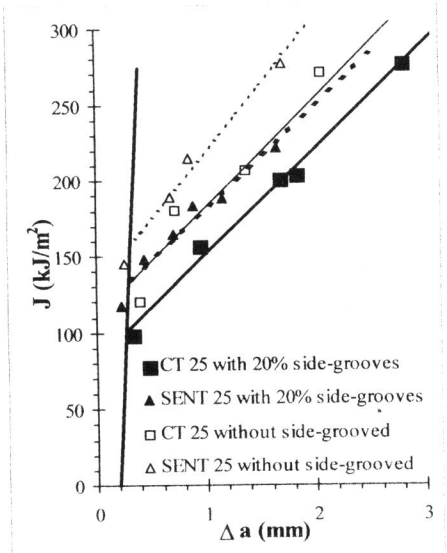

Figure 2 : Geometry and side-grooves effect on J_R-curves.

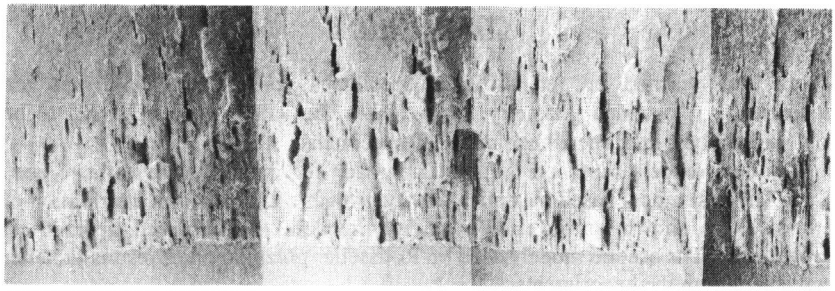

Figure 3 : Scanning electron micrograph showing the presence of delaminations observed on the fracture surface of a CT specimen.

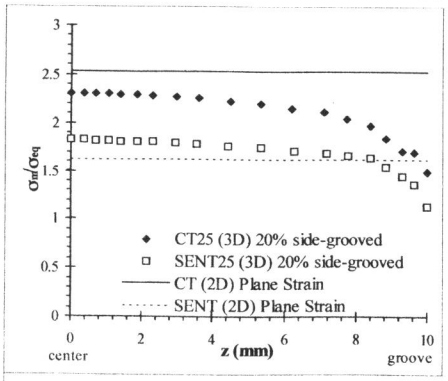

Figure 4 : Variation of the stress triaxiality ratio for different geometries with B=25mm ($J=100kJ/m^2$ and 700μm ahead of the crack tip).

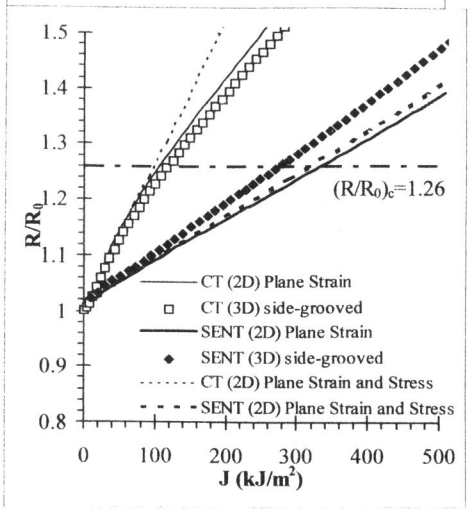

Figure 5 : Variation of the mean cavity growth for different configurations and specimens. The critical cavity growth measured on axisymmetric notched specimens is indicated horizontally.

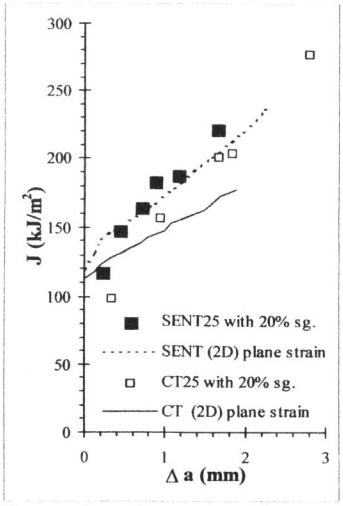

Figure 6 : Comparison between calculated (with Rousselier model) and experimental results (for side-grooved specimens).